Mon. Not. R. Astron. Soc. **000**, 000–000 (2001) Printed 1 February 2008 (MN LATEX style file v2.2)

The relative abundances of ellipticals and starbursts among the Extremely Red Galaxies.

F. Mannucci[1], L. Pozzetti[2], D. Thompson[3], E. Oliva[4,5], C. Baffa[4], G. Comoretto[4], S. Gennari[4], and F. Lisi[4]

[1] *C.A.I.S.M.I. - C.N.R., Largo E. Fermi 5, I-50125, Firenze, Italy*
[2] *Osservatorio Astronomico di Bologna, via Ranzani 1, I-40127, Bologna, Italy*
[3] *Palomar Observatory, California Institute of Technology, MS 320-47, Pasadena, CA 91125*
[4] *Osservatorio Astrofisico di Arcetri, Largo E. Fermi 5, I-50125, Firenze, Italy*
[5] *Centro Galileo Galilei & Telescopio Nazionale Galileo, P.O. Box 565, E-38700, Santa Cruz de La Palma, Spain*

Submitted. Accepted

ABSTRACT

We present J band observations of a complete sample of 57 red galaxies selected to have K′<20 and R−K′>5.3. We use the Pozzetti and Mannucci (2000) prescriptions, based on the R−K and J−K colours, to separate the two dominant populations, old ellipticals and dusty starbursts. We find that both populations are present in the current sample and have similar abundances, and discuss the uncertainties in this result. Galactic stars comprise about 9% of the objects. The starburst galaxies of the present sample are found to give a contribution to the cosmic star formation density similar to the Lyman-break galaxies.

Key words: galaxies: elliptical and lenticular, cD - galaxies: starburst - infrared: galaxies.

1 INTRODUCTION

The Extremely Red Objects (EROs) are galaxies selected to have very red optical-to-IR colours (such as R−K>5.3 or I−K>4). These extreme colours can be due either to an old stellar population in an elliptical galaxy at redshifts between 1 and 2, or to dust reddening of a starburst galaxy or an AGN. Discovered by Elston et al. in 1988, it is still not clear what is the dominant population, and the subject is under active study. Obtaining direct and complete spectroscopic and morphological information is not an easy task because EROs are usually faint at both near-IR and optical wavelengths (K∼19 and R∼ 24). As a consequence, good spectra are available for just a few objects, and no complete sample of EROs has good spectroscopic coverage to date. The limited set of available spectra (e.g., Soifer et al., 1999; Dey et al., 1999; Liu et al., 2000) suggests that both type of objects are present in the ERO population, but the relative abundances remain unknown.

Investigations on the morphology (Moriondo et al., 2000; Treu et al., 1999) and photometric redshifts (Cimatti et al., 1999) of composite samples have produced some evidence that the EROs with K<19 are dominated by elliptical galaxies. The clustering properties of EROs with K<20 (Daddi et al., 2000; McCarthy et al., 2000) are also interpreted as a clue to the presence of more old ellipticals than dusty starbursts.

Recently Pozzetti and Mannucci (2000, hereafter PM2000) introduced a method to statistically separate the two populations by making use of additional observations in the J band. Old stellar populations are expected to show a strong spectral break between 3000 and 5000 Å, while dust reddening of a young population would produce smoother spectra. For redshifts between 1 and 2 this effectively separates the two populations in the R−K vs. J−K colour plane, with starbursts having redder J−K colours. A separation line can therefore be drawn in this colour-colour plane by using predictions from stellar synthesis models and the small number of observed objects with robust classifications. The separation is not very large, about 0.3 mag, so individual objects can be misclassified because of peculiar properties or photometric uncertainties. Nevertheless this method is expected to give reliable statistical information on the relative numbers of ellipticals and starbursts when applied to large enough samples. The colours of the dusty starburst galaxies are not very sensitive to the possible presence of an underlying old stellar population, therefore the objects with composite stellar populations are expected to preferentially fall in the starburst region.

Thompson, Aftreth and Soifer (2000, hereafter TAS2000) observed the field of a radio galaxy at a redshift of

1.47, B3 0003+387, to select EROs by their R−K′ colours. They observed an area of 44.3 sq.arcmin down to a limiting magnitude of K′=20.3. A significant overdensity of red objects is found in this field, in agreement with the strong clustering detected by Daddi et al. (2000). We have observed this field in the J band to classify the objects of this complete sample as ellipticals or starbursts.

Observations and data reduction are described in the following section. Object selection, astrometry and photometry in section 3; in section 4 we present the colour-colour diagram and the relative abundances of the two populations; the uncertainties of the classification are discussed in section 5. In section 6 we derive some consequences on the cosmic star formation history.

2 OBSERVATIONS AND DATA REDUCTION

Observations were obtained at the 3.5m Telescopio Nazionale Galileo (TNG) in the Canary Islands. We used the Near-Infrared Camera and Spectrometer (NICS), a multi-purpose instrument (Baffa et al, 2001) based on a Hawaii 1024×1024 HgCdTe array. The central pixel scale is 0″.253/pix. We used a Js filter, similar to the standard J filter but with a narrower bandpass (1.16 - 1.33 μm) and a higher throughput. We covered the field with many short exposures (1.5 min) for a total integration time of about 3.2 hours. The camera has a field of about $4' \times 4'$, smaller that the TAS2000 selection field of about $7' \times 7'$. Therefore we used a mosaic pattern to observe most of the EROs in the field. The telescope was dithered over three overlapping fields, observed one after the other in order to obtain a final image with a homogeneous PSF and photometric zero point.

We used a two-step reduction procedure. A master sky image was first obtained from a median of all the available images, and subtracted from each frame to obtain a zero-order reduction. The IRAF task DAOFIND was used to detect the 50-100 brightest objects on these subtracted frames to make an object mask. The second step of the procedure makes use of running sky frames using the 6 adjacent exposures, excluding the pixels contained in the object mask. Running sky frames were subtracted from each image, and the results divided by a flat field obtained at sunset.

Precise dithering offsets were measured by selecting a set of about 50 bright compact objects in the first frame and automatically identifying them in the following frames, accounting for the telescope offsets and field distortion. The differences between the recovered positions of these objects in the various images give the offsets, with a typical error of about 0.1″, less than one-half of a pixel.

The distortions from the optics were measured using a crowded stellar field (Hunt and Licandro, priv. comm.), reaching about 3% at the corners of the array. The distortion parameters and the measured offsets were used to drizzle (Fruchter & Hook, 1997) each image onto its final position, creating an undistorted and co-aligned frame for each input image. Given that the PSF is adequately sampled, the results are not very sensitive to the drop size, chosen to be 0.8. The resulting images were combined using a clipped average, which is very efficient at removing cosmic ray hits and residual bad pixels.

The final PSF is about 1.1″ FWHM. An accurate morphological study of the objects far from the field centre is prevented by the PSF degradation due to the aberration of the optics near the edges of the field of view.

The photometric zero point was measured by a set of standard stars from the ARNICA list (Hunt et al., 1998) observed at about the same airmass as the ERO field. We compared the observed R−K′ and J−K′ colours of the stars in the field with the expected colours to check for any error in the zero points. We considered the objects classified as stars by Sextractor (Bertin & Arnouts, 1996; i.e., with a stellarity above 0.9), and compared their colours with those derived by integrating the stellar spectra in the Pickles (1998) library using the same set of filters. A small but systematic difference between the observed and synthetic J−K′ colour of about −0.05 mag was found, and the J-band zero point was corrected accordingly.

The total integration time in each pixel of the final image depends strongly on the pixel position, going from an average value of about 1 hour up to 3 hours in the small region covered by almost all of the images. The detection limit varies accordingly with the integration time. We estimated this limit from the sky noise, after taking into account the correlation between adjacent pixels introduced by the distortion correction. We followed the procedure outlined in Williams et al. (1996), and measured the ratio between the noise in the final image and that in the case of no correlation. The latter was measured on an image constructed without the distortion correction. The correction factor is 1.4, and we used this in eq. 2 of Pozzetti et al. (1998) to estimate the real photometric errors for each object. The measured 5σ detection limit inside an aperture of twice the seeing, 2.2 arcsec, at the positions of the selected EROs (see below) varies between 21.2 and 22.5, with an average of 22.1.

3 OBJECT SELECTION, ASTROMETRY AND PHOTOMETRY

An object catalog down to K′∼20 was made by TAS2000 and the detected objects measured in the R image. The catalog contains magnitudes inside an aperture of 4 arcsec, much larger than the seeing and the intrinsic dimensions of most of the objects of interest in this paper. We corrected the TAS2000 magnitudes for Galactic extinction using the Schlegel et al. (1998) value and the Cardelli et al. (1989) extinction curve. The resulting corrections are 0.215, 0.073 and 0.030 mag in R, J and K′, respectively. Using the (lower) Burstein & Heiles (1982) value for the Galactic extinction would result in R−K′ and J−K′ colours only 0.02 and 0.01 mag redder.

We selected all the objects having R−K′>5.3, which corresponds to the expected colours of an elliptical at z∼1 (see, for example, Cimatti et al., 2000). There are 59 such objects, with K′ magnitudes down to 19.9.

A common coordinate system was established among all the images using the brightest objects, with a resulting r.m.s. positional uncertainty 0.2 arcsec, less than one pixel. This solution was used to derive the expected positions of the EROs in the J band image. 57 of the 59 selected objects are inside the final J band image. The IRAF routine PHOT was used to measure the object flux at these positions inside a circular aperture of 4 arcsec, as in TAS2000. The PSF of

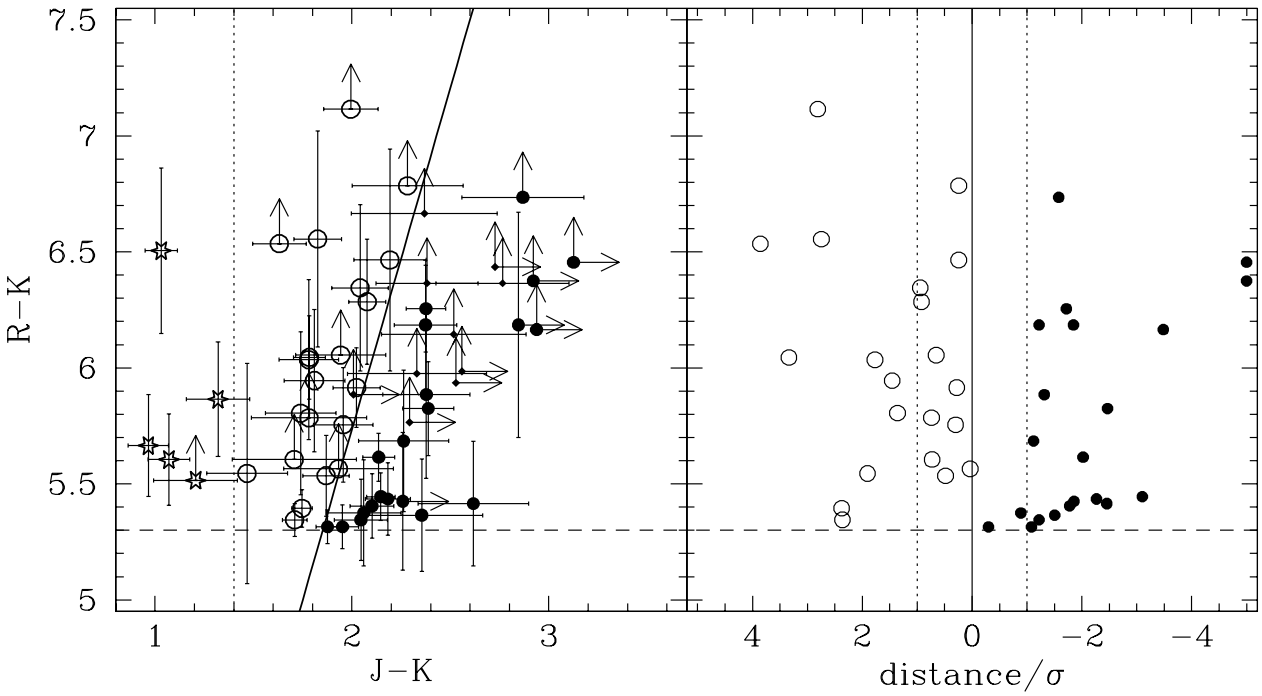

Figure 1. *Left panel*: R−K′ vs. J−K′ colour diagram of the selected EROs. The thick line is the separation between ellipticals and starbursts derived following PM2000. The horizontal dashed line is the colour threshold for selection, the dotted vertical line the J−K′ colour of the separation between stars and galaxies. Open circles represent objects classified as ellipticals, while filled circles represent the starbursts. Stars are used for the stars. Objects with no classification are shown as small diamonds. *Right panel*: significance of the classification as elliptical or starburst. The J−K′ colour of the left panel is replaced with the ratio between the distance of each point from the separation line and the radius of the error ellipse in the direction perpendicular to the line. Objects with a ratio below -5 were plotted at this value. The dotted lines show the 1σ limit of the classification.

all the images are similar, between 0.8 and 1.1 arcsec, and the aperture large enough that the errors on the colours due to differential aperture losses is below 0.05 mag.

4 THE COLOUR-COLOUR DIAGRAM

We computed the expected R−K′ and J−K′ colours of elliptical galaxies and dusty starbursts as in PM2000 for the present filter set: Harris R (0.56 - 0.74 μm), J_s (1.16 - 1.33 μm) and K′ (1.94 - 2.29 μm). The resulting separation line can be described by: $(J - K') = 0.34 \cdot (R - K') + 0.05$. This line is 0.14 mag bluer than in PM2000 mainly because the K′ filter is centred at bluer wavelengths than a standard K filter. Figure 1 shows the position of the objects around this line.

Objects detected in all three bands, and with J−K′ colours redder than the line were classified as starbursts. Bluer objects were classified as ellipticals. A 3σ limiting magnitude was assigned to objects undetected in one band, i.e., with a measured flux below the 3σ uncertainty inside the 4 arcsec aperture. Objects below the separation line but undetected in R, or to the left of the line but undetected in J, were not classified. Objects undetected in R were classified as starbursts if their J−K′ colours were larger than 2.8, corresponding on the separation line to a R−K′ colour of 8. Objects with J−K′<1.4 have colours more typical of M or L dwarf stars (see, for example, Burrows et al., 2001). We therefore classified 5 objects having such colours as stars. The morphology can be reliably studied in four of them (see below), and they are all point sources, confirming this classification. For the final sample of 57 red objects, 21 (37% of the sample) are classified as ellipticals, 21 (37%) as starbursts, 5 (9%) as stars. Ten (17%) remain unclassified. Note that if the two galaxy populations have, on average, different morphology, the relative abundances in any magnitude-limited sample might be affected by different selection effects, especially when the object detection is based on HST data.

Several objects fall near the separation line so that their classification can be affected by the uncertainties on the colours. The significance of the classification was estimated by the ratio of the distance of each point from the classification line divided by the radius of the error ellipse in the direction perpendicular to the line. These results are shown in the right panel of Figure 1. Eleven ellipticals and 2 starbursts have a distance from the line below 1 sigma, therefore their classification should be considered weak.

Figure 1 can also be used to investigate the presence of any correlation between the classification and the R−K′ colour, as proposed by Moriondo et al. (2000) from the morphology. In that case, the most irregular objects tend to show the reddest colours. No such effect is seen in the present sample, but it should be noted that there is only one object with R−K′>7.

5 UNCERTAINTIES AND CHECKS

The PM2000 classification method suffers from some uncertainties that should be accurately discussed and tested.

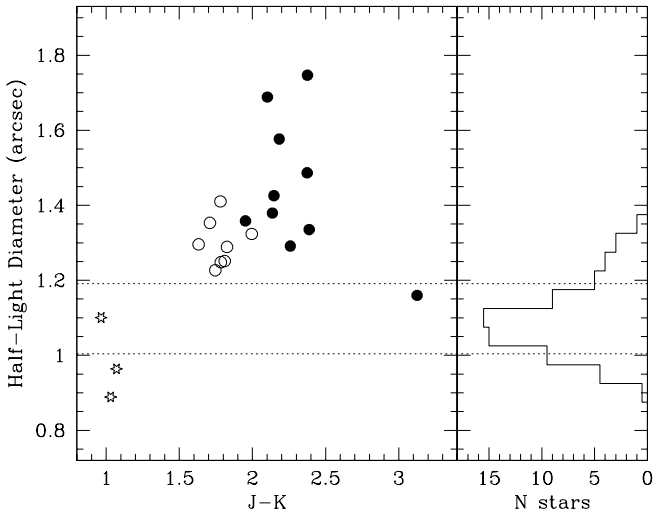

Figure 2. The left panel shows the half-light diameter of the EROs vs. the J−K′ colour. Ellipticals are indicated by open circles, starbursts by solid circles, and stars by open stars. The most extended objects are all classified as starbursts based on their colours. The objects with J−K′∼1 also have compact morphologies. For comparison, the right panel shows the histogram of the half-light diameter for the stars of similar magnitude. The dotted lines are the ±1 sigma limits for the stars.

Many objects in Figure 1 fall near the separation line, at a distance lower than the uncertainties in their colours. Therefore they could easily move from one side of the line to the other because of the measurement errors. While this is a problem for single objects, photometric uncertainties are unlikely to effect the statistical result very much because the density of points on the two sides of the line is similar.

Important systematic effect could be introduced by the uncertainty on the position of the separation line and on the photometric zero point. From the separation of the regions covered by the models (see PM2000) we estimate the former uncertainty to be about 0.1 mag in the J−K′ colour, while the latter is about 0.05 mag. The combined effect of these on the classification can be estimated by moving the line toward bluer or redder J−K′ colours by 0.12 mag: the fraction of ellipticals over starbursts, being 1.0 for the central position of the line, varies from 0.65 and 1.25. In all the cases, the two populations are present at similar levels, within a factor of 35%.

The PM2000 classification methods works for redshifts between 1 and 2. Ellipticals at z>2 are expected to show red J−K colours because the 4000Å break enters into the J band. As a consequence, some of the objects classified as starburst could be ellipticals at redshifts larger than 2. We cannot exclude this for all of the objects, but this is unlikely to be the case for a significant number of starbursts: not many ellipticals at z>2 are expected in a survey this size to K∼20 (see, for example, Cowie et al., 1996).

At redshifts below 1, the 4000Å break of the elliptical galaxies is inside the R filter bandpass. The galaxies then have bluer R−K′ colours and tend to be excluded from the colour-selected sample. Nevertheless, old galaxies at z<1 can be selected if they have metallicities larger than solar, making the colours redder, or if some dust is present. By making use of the Bruzual and Charlot models (1993, version 2000) it is possible to see that ellipticals with metallicities 2.5 times solar at z∼0.8 could populate the colour-colour diagram in the lower-left part of the starburst region (R−K′∼5.5 and J−K′∼ 2) and be misclassified. It is not possible to exclude that this is the case for some of the objects in this part of the diagram, and this is one of the largest uncertainties for this method. Nevertheless the morphological information (see below) implies that this is not a dominant contribution: three of the objects in this region of the diagram are among the most extended.

The morphology of the selected objects can be used as a check of the classification method. The galaxies with compact morphologies can be both ellipticals and starbursts, but we expect that the most extended or disturbed objects will have the colours of a dusty starburst galaxy.

The spatial extent of the objects was measured on the TAS2000 K′ image, more appropriate than our J band image because it has lower aberrations. We have extracted the value of the half-light radius from the Sextractor catalog both for the EROs and for the stars. All the objects with formal error on the K′ magnitude larger than 0.10 mag (signal-to-noise ratio lower than about 10) or with weak classification (distance from the separation line in Figure 1 less than 1 sigma) were excluded. The results for the remaining 23 objects are shown in Figure 2, where the half-light diameter of each objects is plotted versus the J−K′ colour. As expected, the most extended objects have starburst colours. Some of the ellipticals with weak classifications (and therefore not shown in Figure 2) show extended morphologies: these objects could be misclassified starbursts or objects with composite stellar populations. It can also be seen that all the objects in Figure 2 with J−K′∼1 also have compact morphologies, a strong indication that they are M or L dwarf stars.

6 THE COSMIC STAR FORMATION HISTORY

The number of the starburst galaxies selected by the survey and their individual SFRs could be used to derive the contribution to the cosmic star formation history from this class of galaxies. This is potentially very important as the current estimates are based on search techniques that would miss this population. Many techniques to select galaxies at z>2 are based on the rest-frame UV or blue continuum, and therefore tend to exclude dusty galaxies. Most of the objects were selected by detecting a blue continuum and the Lyman break (e.g., Steidel et al, 1999). As illustrated in Figure 3, any galaxy with E(B−V) larger than about 0.3 would escape the selection criterion because of the lack of a very blue continuum. Very active, dusty galaxies can be selected by SCUBA at sub-mm wavelengths (e.g., Hughes, 1998). In this case there is a lower limit rather than an upper limit in the extinction, but the minimum SFR that can be detected at redshifts between 1 and 2 are around a few hundred solar masses per year (see, for example, Ivison et al., 2000). These techniques are not sensitive to moderately active (20<SFR<100 $M_\odot$/yr), moderately dusty (0.3<E(B−V)<0.8) galaxies, the population that can be selected as EROs.

To derive a reliable value for the star formation density

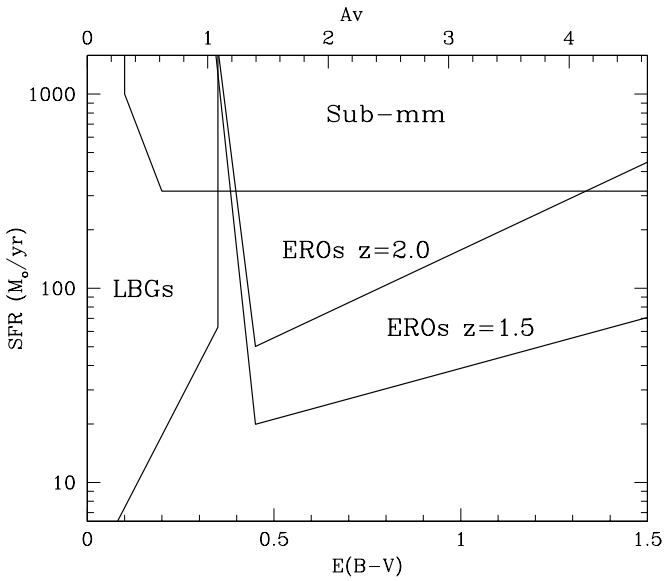

Figure 3. Regions of the SFR - extinction plane that can be selected by the various search techniques. Sub-mm observations can currently detect galaxies with any extinction but with very high SFRs. Lyman-break galaxies (LBG) must have E(B−V) below about 0.3, but can have low SFRs. The ERO technique covers a region of this plane with E(B−V) between 0.5 and 1 and a star formation rate down to about 20 $M_\odot$/yr. The exact values of the edges depend on many assumptions, such as the choice of telescope and instrument, the integration time, dust temperature, and redshift. Therefore the limits should be regarded only as indicative. Only methods aimed to detect the continuum are shown; techniques targeting emission lines are not included in the plot.

is beyond the aim of this paper. Many large uncertainties prevent us from this: the redshift distribution of the objects is not known; it is difficult to estimate the exact cosmic volume sampled by the broad-band selection; the SFRs cannot be precisely derived from the limited set of available colours; even if observations at many wavelength were present, the value of the SFR is usually not well constrained as it is very sensitive to the unknown star-formation history, IMF, extinction law and amount of dust.

With these problems in mind, we derive an order-of-magnitude estimate of the star formation density. We assume that all the starbursts are at redshifts between 1 and 1.5. The first limit is due to the colour selection, while the second comes from the luminosity limit. The RJK colours can be reproduced by models of starburst galaxies in this redshift range with SFRs between 20 and 100 $M_\odot$/yr and E(B−V) between 0.5 and 1.0. Adding the SFRs of the 21 galaxies in the present sample and dividing the result for the sampled volume of about 53000 Mpc^3 (H_0=50 Km/sec/Mpc, $\Omega_m = 1$, $\Omega_\Lambda = 0$), we obtain a cosmic star formation density of about 0.03 $M_\odot$/yr/Mpc^3; a similar value is obtained with H_0=70, $\Omega_m = 0.3$ and $\Omega_\Lambda = 0.7$. This value is very similar to that observed at higher redshift in the Lyman Break galaxies (e.g., Steidel et al., 1999). The uncertainties are too large to place any reliable constraints on the galaxy formation models, and the contribution from all the fainter undetected galaxies is not known. Nevertheless this is an indication that the ERO technique is not only a good method to detect high-redshift ellipticals, but also a promising way to select a population of starburst galaxies containing a significant fraction of star formation and having intermediate properties between the Lyman-break galaxies and the SCUBA objects.

We are grateful to L. Hunt and J. Licandro for providing the NICS distortion parameters, to the TNG staff for support during the observations and to L. Testi for discussion about brown dwarfs.

The object catalog can be obtained in electronic form from the web site: www.arcetri.astro.it/∼filippo/RJK

REFERENCES

Baffa, C., et al., 2001, A&A, in press.
Bertin, E., and Arnouts, S., 1996, A&AS, 117, 393
Bruzual, G., and Charlot, S., 1993, ApJ 405, 538
Burrows, A., Hubbard, W.B., Lunine, J.I., and Liebert, J., 2001, in press (astroph0103383)
Burstein D., and Heiles C. , 1982, AJ, 87, 1165
Cardelli, J. A., Clayton, G. C., and Mathis, J. S.; 1989, ApJ, 345, 245
Cimatti, A. et al., 1999, A&A, 352L, 45
Cimatti, A., Villani, D., Pozzetti, L., and di Serego Alighieri, S., 2000, MNRAS 318, 453
Cowie, L., L., Songaila, A., Hu, E. M., and Cohen, J. G., 1996, AJ, 112, 839
Daddi, E., Cimatti, A., Pozzetti, L., Hoekstra, H., Rottgering, H.J.A., Renzini, A., Zamorani, G., and Mannucci, F., 2000, A&A 361, 535
Dey, A. , Graham, J. R., Ivison, R. J., Smail, I. , Wright, G. S. and Liu, M. C. 1999, ApJ, 519, 610
Elston, R., Rieke, M. J., and Rieke, G. H., 1988, ApJ 341, 80
Fruchter, A., and Hook, R.N., 1997, SPIE 3164, 120
Hughes, D. H., et al., 1998, Nature, 394, 241
Hunt, L. K., Mannucci, F., Testi, L., Migliorini, S., Stanga, R. M., Baffa, C., Lisi, F., and Vanzi, L., 1998, AJ 115, 2594
Ivison, R. J., Smail, I., Barger, A. J., Kneib, J.-P., Blain, A. W., Owen, F. N., Kerr, T. H., and Cowie, L. L., 2000, MNRAS 315, 209
Liu, M.C., Dey, A., Graham, J.R., Bundy, K.A., Steidel, C.S., Adelberger, K., and Dickinson, M.E., 2000, AJ 119, 2556
McCarthy, P., et al., 2000, in press, (astro-ph/0011499)
Moriondo, G., Cimatti, A., and Daddi, E., 2000, A&A 364, 26
Pickles, A. J., 1998, PASP, 110, 863
Pozzetti L., Madau, P., Zamorani, G., Ferguson, H. C., and Bruzual, G., 1998, MNRAS 298, 1133
Pozzetti, L., and Mannucci, F., 2000, MNRAS, 317, L17 (PM2000)
Schlegel, D. J., Finkbeiner, D. P., and Davis, M. 1998, ApJ, 500, 525
Soifer, B. T., Matthews, K., Neugebauer, G., Armus, L., Cohen, J. G., Persson, S. E. and Smail, I. 1999, AJ, 118, 2065
Steidel, C. C., Adelberger, K. L., Giavalisco, M., Dickinson, M., and Pettini, M., 1999, ApJ, 519, 1
Thompson, D., Aftreth, O., and Soifer, B. T., 2000, AJ, 120, 2331 (TAS2000)